Biomass Conversion and Biorefinery (2024) 14:5651–5664
https://doi.org/10.1007/s13399-022-03677-6

ORIGINAL ARTICLE

Red pepper (*Capsicum annuum* L.) industrial processing pulp-derived nanoporous carbon sorbent for the removal of methylene blue, diclofenac, and copper(II)

Filiz Koyuncu[1] · **Fuat Güzel**[2] · **Yekbun Avşar Teymur**[1]

Received: 5 October 2022 / Revised: 3 December 2022 / Accepted: 13 December 2022 / Published online: 17 January 2023

Abstract
The present study relates to the physicochemical investigation of the methylene blue, diclofenac, and copper(II) sorptions from the water of the new activated carbon (RPAC) prepared in single-step KOH-activated pyrolysis from red pepper (*Capsicum annuum* L.) industrial processing pulp (RP) under optimized conditions. Sorption conditions were optimized according to the maximum effects of key factors (RPAC dosage, sorbate concentration, interaction time, and temperature) affecting sorption processes at their natural pH in water. The kinetic and equilibrium experimental sorption data of the examined sorbates were simulated to widely used models and found to fit well with the pseudo-second-order and Langmuir models, respectively. The maximum sorption capacity for methylene blue, diclofenac, and copper(II) by RPAC was found to be 322.6, 303.0, and 196.1 mg g^{-1} at their natural pH and 50 °C, respectively. Thermodynamic parameters determined for each sorption system indicated that the sorption processes were endothermic and spontaneous. The outputs of the present study highlight that RPAC can be used as an effective sorbent in removing contaminants from water.

Keywords Red pepper pulp · Activated carbon · Water treatment · Sorption · Reusability

1 Introduction

In recent decades, the number of pollutants discharged into water systems has been increasing from industries with *growing* demands as a result of the rapid increase in the world population. Generally, water pollutants such as heavy metals, drugs, dyes, pesticides, petroleum products, and water-soluble inorganic and organic substances cause serious problems as they can affect the ecosystem and threaten the health of living organisms due to their toxic effects. Therefore, recently, scientists have increased their efforts to develop more effective new methods to treat wastewater [1, 2].

✉ Filiz Koyuncu
flkync@gmail.com

✉ Fuat Güzel
fguzel@dicle.edu.tr; guzelfuat@gmail.com

[1] Department of Chemistry, Institute of Natural and Applied Sciences, Dicle University, Diyarbakir 21280, Turkey

[2] Department of Chemistry, Faculty of Education, Dicle University, Diyarbakır 21280, Turkey

Various physical, chemical, and biological water treatment methods are applied to remove water contaminants. Although most of these methods are quite effective, they are rarely applied due to the disadvantages of being quite expensive and creating secondary pollutants [3–5]. Therefore, low-cost and high-efficient method research has become the focus of the scientific world. Among these methods, the sorption method is commonly used in the remediation of polluted water due to its ease of use, high efficiency, low operating cost, and reliability compared to other methods [6, 7]. The effectiveness of this method depends on the textural features such as porosity and internal surface area as well as the surface chemical features of the sorbent [8]. In this context, carbonaceous porous sorbents, especially activated carbons (ACs), have a very important place among sorbents [9]. They, which have properties such as chemical inertness, large porosity, high specific surface area, and good thermal stability, have been successfully applied from an undetermined date to the present in various fields such as water treatment, gas separation, environmental remediation, catalyst support, energy storage, pharmacology, and gas storage [10, 11]. They are produced by pyrolysis by one- and two-stage physical activation in the existence of oxidizing gases

such as carbon dioxide, air, steam, and chemical activation of the precursors used with chemical agents such as alkali hydroxides, inorganic acids, and alkali carbonates [12–14]. Different precursors such as lignite, coconut, wood, peat, and coal are often used in commercial AC production. However, since they are not available everywhere, the shipping cost increases the cost of AC production and limits their use as precursors [15, 16]. In recent decades, there has been increasing use of agricultural and agro-industrial wastes, which are abundantly available, renewable, inexpensive, and sustainable, as a precursor to reducing the cost of AC production [17, 18]. Since biomass wastes such as agricultural wastes, forest residues, industrial wastes, animal wastes, and municipal solid wastes are renewable, widely available, inexpensive, and environmentally friendly resources, their effective use in the production of AC by thermochemical conversion attracts increasing attention all over the world [19]. The production of ACs based on circular economy criteria, especially by using industrial processed food waste, is a very important approach for sustainable global development [20].

According to our literature review, no studies have been performed on the removal of methylene blue, diclofenac, and copper(II) ions with AC (RPAC) produced under optimum production conditions by single-step KOH-activated pyrolysis from red pepper industrial processing pulp (RP). Methylene blue, diclofenac, and copper(II) ions are among the most emerging water pollutants in wastewater treatment plant influent, effluent, surface water, and drinking water, which is why they are frequently used as model sorbate to test the pollutant sorption performance of a prepared sorbent. Methylene blue is a water-soluble cationic dyestuff. Acute exposure to it has been reported to cause increased heart rate, vomiting, shock, Heinz body formation, cyanosis, jaundice, quadriplegia, and tissue necrosis in humans [21]. Diclofenac is a drug with the highest acute toxicity among non-steroidal anti-inflammatory drugs [22]. It has been reported to cause severe visceral gout or renal failure in humans even at low concentrations due to its non-easily biodegradable and aquatic ecotoxic properties. It is one of the most common heavy metal pollutants in the environment with the highest toxicity to living organisms [23].

The specific objectives of the present study are to (i) examine the sorptive performance of RPAC with physicochemical parameters for the elimination of methylene blue, diclofenac, and copper(II) in water; (ii) determine the optimum sorption conditions according to the effects of the key process variables (i.e., RPAC dosage, initial sorbate concentration, interaction period, and solution temperature) at the natural pH of each sorption system; (iii) model sorption kinetics and isotherm data for each sorbate; (iv) elucidate the sorption mechanisms of sorbates by comparing Fourier transform infrared (FT-IR) and scanning electron microscopy-energy dispersive X-ray (SEM–EDX) spectroscopic analyses of RPAC before and after sorption; and (v) test the reusability stability of RPAC by cyclic sorption/desorption studies for each sorbate.

2 Materials and methods

2.1 Materials

RPAC was produced by one-step KOH-activated pyrolysis of red pepper pulp (RP) supplied from a local pepper paste factory in Diyarbakır, Turkey. The influence of production variables, some physicochemical characterizations, and cost estimation are mentioned in our previous study. Some of its important physicochemical properties are listed in Table 1 [24]. Methylene blue (chemical formula, $C_{16}H_{18}ClN_5S$; molecular weight, 319.9 g mol^{-1}; ionization, basic; chemical class, cationic dye; maximum wavelength, 665 nm), diclofenac (chemical formula, $C_{14}H_{10}Cl_2NNaO_2$; molecular weight, 296 g mol^{-1}; chemical class, non-steroidal anti-inflammatory drug; maximum wavelength, 276 nm) and copper (molecular weight, 63.5 g mol^{-1}; chemical class, transition metal) were provided from the distributor of Sigma-Aldrich Co. in Ankara, Turkey, and used as original without any processing. Artificial solutions at the desired concentration for each sorbate were prepared with appropriate dilutions with ultrapure water from their stock solutions of 1000 mg L^{-1}.

2.2 Batch sorption and desorption studies

Batch sorption experiments were accomplished by stirring at 150 rpm for the needed time in a water bath with a temperature-controlled shaker (J.P. Selecta, Spain) of 100 mL Erlenmeyer containing a 50 mL solution of known concentrations of the sorbates. Optimum sorption conditions were decided by investigating the effects of some operating parameters

Table 1 Physical and chemical characteristics of RPAC [24]

Textural characteristics		Surface chemical characteristics	
S_{BET} (m^2 g^{-1})	1564	Carboxylic (mEq g^{-1})	0.48
V_T (cm^3 g^{-1})	0.623	Phenolic (mEq g^{-1})	0.18
V_{mic} (cm^3 g^{-1})	0.570	Lactonic (mEq g^{-1})	0.42
V_{mes} (cm^3 g^{-1})	0.053	Total acidity (mEq g^{-1})	1.08
V_{mic} (%)	90.7	Total basicity (mEq g^{-1})	1.05
V_{mes} (%)	9.3	pH_{PZC}	5.78
D_P (nm)	1.8		

†S_{BET}, BET surface area; V_T, total pore volume; V_{mic}, micropore volume; *V*mes, mesopore volume; V_{mic} (%), micropore fraction; V_{mes} (%), mesopore fraction; D_P, average pore diameter; pH_{PZC}, point of surface zero charge

on their sorption by varying the studied parameters such as RPAC amount (50–100 mg), initial sorbate concentration (300, 400, and 500 mg L^{-1}), interaction time (0–380), and temperature (20, 30, 40, and 50 °C) at natural pH (7.0 for methylene blue, 4.9 for diclofenac, and 5.0 for copper(II) level in water of each sorbate studied by retaining the others constant). The concentrations of the sorbates used before and after sorption were measured with UV–Vis (Perkin Elmer-Lamda 25, USA) and atomic absorption (PerkinElmer AAnalyst, 100A) spectrophotometers.

For kinetic experiments, 50 mg of RPAC was mixed with 50 mL of each sorbate solution with initial concentrations of 300, 400, and 500 mg L^{-1}, a temperature of 25 °C, and a shaking speed of 150 rpm at the natural pH of each RPAC-sorbate sorption system. At the indicated time intervals (0–380 min), 10 mL of samples was removed and filtered. The amount (q_t, mg g^{-1}) sorbed at any time t (min) was calculated from Eq. (1):

$$q_t = \left(C_i - C_t\right)V/m \tag{1}$$

where C_i (mg L^{-1}) is the initial sorbate concentration, C_t (mg L^{-1}) is the concentration of sorbate at any time, V (L) is the volume of solution, and m (g) is the mass of sorbent.

Equilibrium isotherm experiments were performed at 20, 30, 40, and 50 °C temperatures using solutions of various concentrations of the sorbates under optimized sorption conditions previously determined at the natural pH of each sorbate sorption system. Thesorption capacity (q_e, mg g^{-1}) per gram of sorbent at equilibrium was calculated from Eq. (2):.

$$q_e = \left(C_i - C_e\right)V/m \tag{2}$$

Where C_e (mg L^{-1}) is the equilibrium concentration of sorbate in the solution.

Determining the kinetic and isotherm model best suited to the sorption systems examined was determined by proximity to the unit and zero, respectively, of the regression coefficient (R^2) and normalized standard deviation (Δq, %) values computed with Eqs. (3) and (4) [25]:

$$R^2 = 1 - \left[\sum_{i=1}^{n}\left(q_{e,exp} - q_{e,cal}\right)^2 / \sum_{i=1}^{n}\left(q_{e,exp}\right)^2 - \left(\left(\sum_{i=1}^{n} q_{e,exp}\right)^2 / n\right)^2\right] \tag{3}$$

$$\Delta q(\%) = 100\sqrt{\sum_{i=1}^{n}\left[\left(q_{e,exp} - q_{e,cal}\right)/q_{e,exp}\right]^2 / N - 1} \tag{4}$$

where $q_{e,cal}$ and $q_{e,exp}$ represent the calculated and experimentally determined sorbed amounts of sorbate, respectively. N is the experimental data number. In addition, the compatibility comparison of $q_{e,cal}$ and $q_{e,exp}$ values determined from the kinetic models was also taken into account in the kinetic modeling [26].

Surface physical morphology, elemental composition, and organic functional groups of RPAC before and after sorption of each sorbate were identified by using SEM–EDX and FT-IR spectroscopic techniques. SEM–EDX analyses were performed by using an SEM–EDX device (Supra 40VP, Zeıss, Germany). FT-IR spectrum was recorded with a spectrophotometer (PerkinElmer spectrum 100) through attenuated total reflectance (ATR) using 16 cm^{-1} resolutions in the range of 4000–450 cm^{-1}.

Batch desorption cycle experiments were performed with different eluents such as HCl, H_2SO_4, NaOH, and C_2H_5OH with various concentrations and distilled H_2O to test the reusability of spent RPAC after sorption of the investigated sorbates. To this end, firstly, the sorption of the investigated sorbates on the RPAC was accomplished by shaking Erlenmeyer including 50 mg of RPAC and 50 mL sorbate solutions of 50 mg L^{-1} concentration at a shaking speed of 150 rpm and at 25 °C and their natural pH for 1 h in a shaking water bath. The spent RPAC after each sorbate sorption was removed from the solution medium by filtering the solutions and dried at 105 °C overnight. Then, it was shaken for 6 h with the solutions of the eluents used to determine the eluent that was effective in eliminating the sorbate from the RPAC surface. Sorbed and desorbed concentrations of sorbate in the supernatant were measured as described above. These experiments were carried out in triplicate under the same conditions and averaged. Desorption studies were repeated in five cycles to determine the reusability efficiency of RPAC for each sorbate. The sorption and desorption efficiencies were calculated from Eqs. (5) and (6) equations, respectively:

$$Sorptionefficiency(\%) = \left(C_i - C_e/C_i\right)100 \tag{5}$$

$$Desorptionefficiency(\%) = \left(q_d/q_a\right)100 \tag{6}$$

where q_d and q_a (mg g^{-1}) indicate the sorbed and desorbed amounts of the sorbate, respectively.

3 Results and discussions

3.1 Effects of sorption variable–sorption optimization

3.1.1 Effect of RPAC dosage

The effect of RPAC dose on the sorption of used sorbates was investigated by adding different dosages of RPAC (ranging from 50 to 100 mg) into 50 mL of a sorbate solution of 300 mg L^{-1} concentration in 100 mL of capped Erlenmeyer at 25 °C and is shown in Fig. 1. The sorbed amount of methylene blue, diclofenac, and copper(II) ions by increasing the

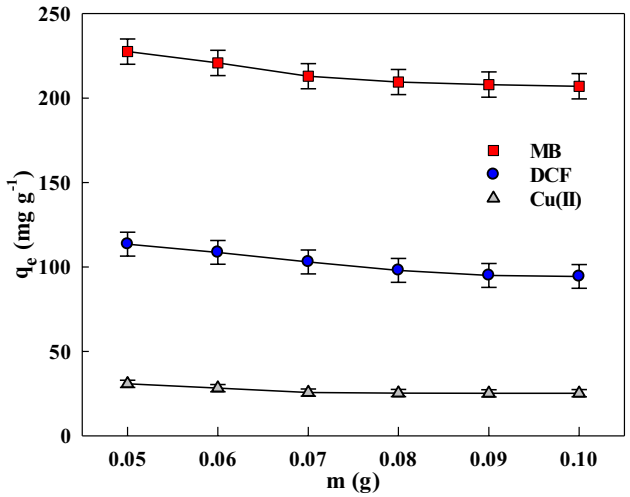

Fig. 1 Effect on the sorption of methylene blue (MB), diclofenac (DCF), and copper (Cu(II)) of RPAC dosage (initial sorbate concentration, 300 mg L.$^{-1}$; pH, 7.0 for methylene blue, 4.9 for diclofenac, and 5.0 for copper(II); interaction period, 240 min for methylene blue, 260 min for diclofenac, and 80 min for Cu(II); temperature, 25 °C)

dose of RPAC from 50 to 100 mg decreased from 235.5 to 216.7 mg g^{-1}, from 114.2 to 107.2 mg g^{-1}, and from 33.3 to 22.9 mg g^{-1}, respectively. This reduction may be due to the progressive reduction of active sites for sorption on its surface as a result of surface overlap with increasing dosage. Similar observations and comments were also emphasized in previous studies [27–29]. The optimum RPAC dosage was chosen as 50 mg for subsequent sorption studies of each sorbate.

3.1.2 Effects of interaction period/initial sorbate concentration–kinetic modeling and diffusion mechanism

Figure 2 demonstrates the effect of the interaction period/initial sorbate concentration on the sorption of used sorbates by RPAC. The sorption of each sorbate was fast at the beginning and then reached equilibrium with a slight increase. The fact that the rate of sorption is fast at first and then slower is probably due to the presence of active binding sites on the surface and slow pore diffusion of the sorbate ions into the mass of the sorbent, respectively [30]. The sorption of methylene blue, diclofenac, and copper(II) ions reached equilibrium at 240, 260, and 80 min, respectively, and was chosen as the equilibrium interaction time for their further sorption experiments. The sorption capacity of methylene blue, diclofenac, and copper(II) ions at equilibrium increases from 192.5 to 270.3 mg g^{-1} and from 122.8 to 141.3 mg g^{-1} and from 28.2 to 51.3 mg g^{-1}, respectively, by increasing from 200 to 400 mg L^{-1} of the initial sorbate concentration. These increases are most likely due to an increase in the driving force of the concentration gradient with an increase in the initial sorbate concentration [31, 32].

For kinetic modeling of each sorption system, kinetic data of each sorbate in Fig. 2 were evaluated in the widely used pseudo-first-order (PFO) [33] and pseudo-second-order (PSO) [34] kinetic models, and their linearized equations are given in Eqs. (7) and (8):

$$PFO: \ln\left(q_e - q_t\right) = \ln q_e - k_1 t \tag{7}$$

$$PSO \ t/q_t = 1/k_2 q_e^2 + \left(1/q_e\right)t \tag{8}$$

where q_e (mg g^{-1}) is the sorbed amount at equilibrium, q_t (mg g^{-1}) is the sorbed amount at time t, k_1(1/min) is PFO rate constant, and k_2 (mg g^{-1} min^{-1}) is PSO rate constant.

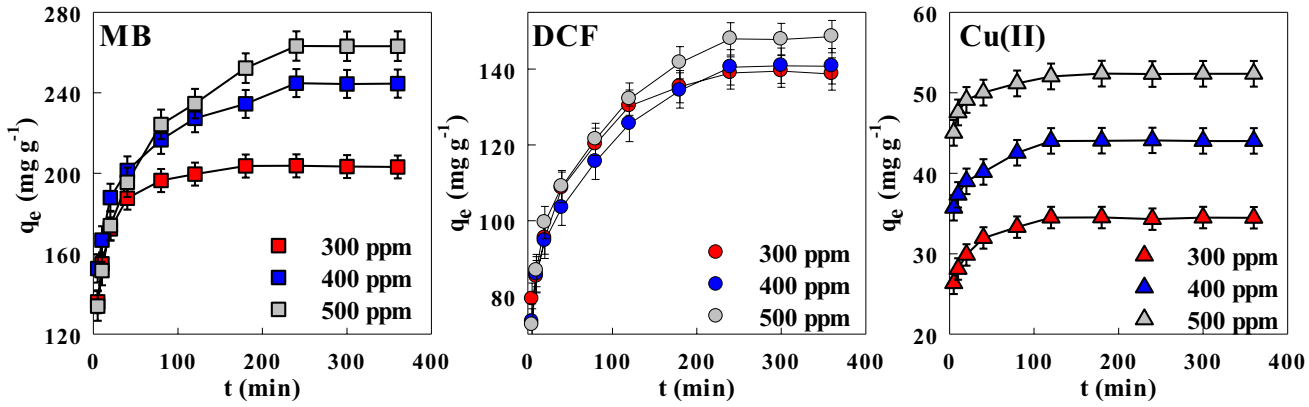

Fig. 2 Effect of interaction time/initial sorbate concentration on the MB, DCF, and Cu(II) sorption capacity of RPAC (RPAC dosage, 50 mg; pH, 7.0 for methylene blue, 4.9 for diclofenac, and 5.0 for copper(II); temperature, 25 °C)

Table 2 Kinetic parameters of methylene blue, diclofenac, and copper(II) sorption onto RPAC

Model		Pseudo-first-order				Pseudo-second-order					Intra-particle diffusion			
C_i	$q_{e,exp}$	$q_{e,cal}$	k_1	R^2	$\Delta q\%$	$q_{e,cal}$	k_2	R^2	$\Delta q\%$	h	k_{id}	I	R^2	$\Delta q\%$
Methylene blue														
300	203.6	56.7	2.4	0.9556	5.78	204.1	1.5	0.9999	1.72	63.3	2.6	167.3	0.9656	8.61
400	244.8	80.6	1.2	0.9733	4.86	237.5	0.8	0.9991	1.11	44.6	4.7	171.4	0.9772	5.70
500	263.3	124.5	1.3	0.9896	3.60	256.4	0.4	0.9969	0.99	28.3	6.3	173.2	0.9716	4.04
Diclofenac														
300	139.0	61.9	1.6 0.9972	6.77	138.9	0.9	0.9976	2.55	17.0	3.4	47.0	0.9413 7.33		
400	140.5	64.9	1.3 0.9918	3.98	136.0	0.8	0.9956	1.83	15.3	4.8	73.1	0.9796 4.91		
500	148.0	71.2	1.3 0.9888	3.01	144.9	0.7	0.9957	0.78	15.1 11.9	91.4	0.9820	3.78		
Copper(II)														
300	34.5	8.2	2.5 0.9790	4.88	34.1 13.4	0.9997 1.82		55.3	0.4	28.6	0.9896	6.65		
400	44.0	8.6	2.2 0.9876	3.22	43.1 13.1	0.9993 1.25		24.3	0.5	34.4	0.9798	5.24		
500	52.0	6.2	2.2 0.9271	2.67	51.6 20.8	0.9999 0.75		15.6	0.9	47.3	0.9897	2.99		

†C_i, mg L^{-1}; $q_{e,exp}$, mg g^{-1}; $q_{e,cal}$, mg $^{-1}$; $k_1 \times 10^{-2}$, min^{-1}; k_2 $^{-10-3}$, g mg^{-1} min^{-1}; k_{id}, mg g^{-1} $min^{-1/2}$; C, mg g^{-1}; h, mg g^{-1} min^{-1}

In addition, the initial sorption rate (h, mg g^{-1} min^{-1}) was calculated from Eq. (9) [35]:

$$h = k_2 q_e^2 \tag{9}$$

The kinetic parameters, R^2, and $\Delta q(\%)$ values for each sorbate were determined from the plots (Fig. S1) drawn according to the linearized equation of the PFO ($log(q_e - q_t)$ vs. t) and PSO (t/q_t vs. t) kinetic models and are given in Table 2. The R^2 and Δq (%) values determined from the PSO kinetic model for all three sorbates are closer to one and to zero than the PFO, respectively. Accordingly, the PSO kinetic model is more appropriate to define the sorption kinetics of the sorbates studied onto RPAC. It also confirms that the $q_{e,cal}$ and $q_{e,exp}$ values calculated by the PSO kinetic model are much closer than those of the PFO kinetic model. In addition, k_2 values decrease with increasing the initial concentration of used sorbates. This is most likely because the affinity between the sorbate ions and the surface decreases with the decrease of active centers on the RPAC surface with increasing sorption with increasing initial sorbate concentration. Also, the initial sorption rate, h, calculated from Eq. (9) for the used sorbates decreases with increasing initial sorbate concentration. This decrease is possibly due to the sorbate ions, which are concentrated in a unit volume with increasing concentration, preventing the orientation of one another to the sorbent surface.

PFO and PSO kinetic models cannot elucidate the diffusion mechanism of a sorption process. Therefore, kinetic data are assessed in the equation of the intra-particle diffusion (IPD) model based on the theory proposed by Weber–Morris [36]. This model is described by the equation given in Eq. (10):

$$q_t = k_{id} t + C \tag{10}$$

where the k_{id} (mg g^{-1} $min^{-1/2}$) is the IPD rate constant and I (mg g^{-1}) is the thickness of the boundary layer between sorbent–sorbate in a sorption system. If the I value is zero or close to zero in a sorption process, it implies that the rate-controlling stage is only the IPD stage or it is more dominant than the other stages, respectively [37]. Furthermore, the graph of q_t versus $t^{1/2}$ gives a straight line through the origin that the rate-controlling stage in a sorption mechanism is only the IPD stage; otherwise, there is a complex mechanism affected by the other stages mentioned above [38].

The kinetic data in Fig. 2 of each sorbate was evaluated in Eq. (10), and IPD plots were drawn and shown in Fig. 3. This figure shows that they are non-linear in the whole time range, which shows that the rate-controlling stage in the sorption of all three sorbates is not only the IPD stage but a complex mechanism in which the above-mentioned stages are also effective. k_{id} and I values for different initial concentrations of each sorbate were calculated from the slope and intersection points of the second linear portion of curves in Fig. 3, respectively, and are given in Table 2. The k_{id} values increase with the increase in the initial concentration. This is probably due to an increase in the driving force of the sorbate ions to the sorbent pores with increasing initial sorbate concentration. It is also seen that I values are greater than zero and increase with increasing initial sorbate concentration. This fact approves that the rate-controlling stage in the sorption process is not only the IPD stage but may contribute to other stages [39].

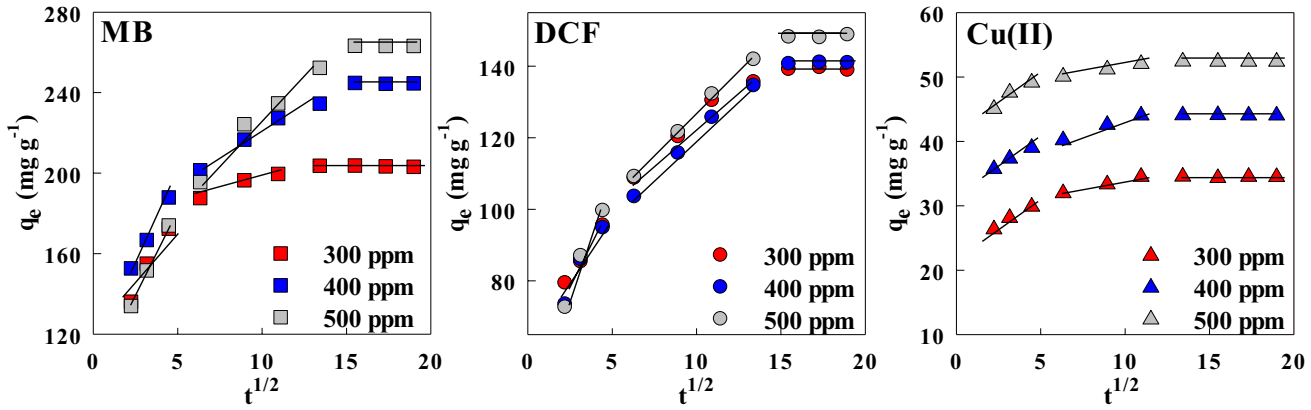

Fig. 3 Intra-particle diffusion plots for MB, DCF, and Cu(II) sorption of RPAC

3.1.3 Effect of temperature–isotherm modeling and thermodynamic analysis

Figure 4 displays the temperature effect on the sorption of the used sorbates by RPAC. The methylene blue, diclofenac, and copper(II) sorption capacity of RPAC by increasing the temperature from 20 to 50 °C increased from 238.3 to 317.6 mg g^{-1}, from 191.10 to 270.9 mg g^{-1}, and from 82.1 to 114.3 mg g^{-1}, respectively, pointing that their sorption process is endothermic. This increase is probably due to the increase in the diffusion rate of sorbate ions to the surface and pores of the sorbent as a result of decreasing viscosity with increasing solution temperature [40].

For isotherm modeling, the isotherm data at 20, 30, 40, and 50 °C temperatures in Fig. 4 of each sorbate were evaluated in the widely used Langmuir [41] and Freundlich [42] isotherm models. The linearized equations of these models are as in Eqs. (11) and (12):

$$Langmuir\ \ C_e/q_e = 1/q_m K_L + \left(1/q_m\right)C_e \tag{11}$$

$$Freundlich\ \ \ln q_e = \ln K_F + \left(1/n_F\right)\ln C_e \tag{12}$$

where q_m (mg g^{-1}) is the maximum sorption capacity, K_L (L mg^{-1}) is the Langmuir equilibrium constant, K_F ((mg g^{-1}) (L mg^{-1})$^{1/n}$) is the Freundlich constant, and n is the heterogeneity factor. If $1/n_F$ is less than and greater than one, it indicates that the sorption process is favorable and unfavorable, respectively [43].

Also, Langmuir's dimensionless separation factor (R_L) was calculated from Eq. (13) to predict the adsorption tendency:

$$R_L = 1/\left(1 + K_L C_i\right) \tag{13}$$

If the R_L value is less than or greater than unity, the sorption process is assumed to be favorable and unfavorable, respectively [44].

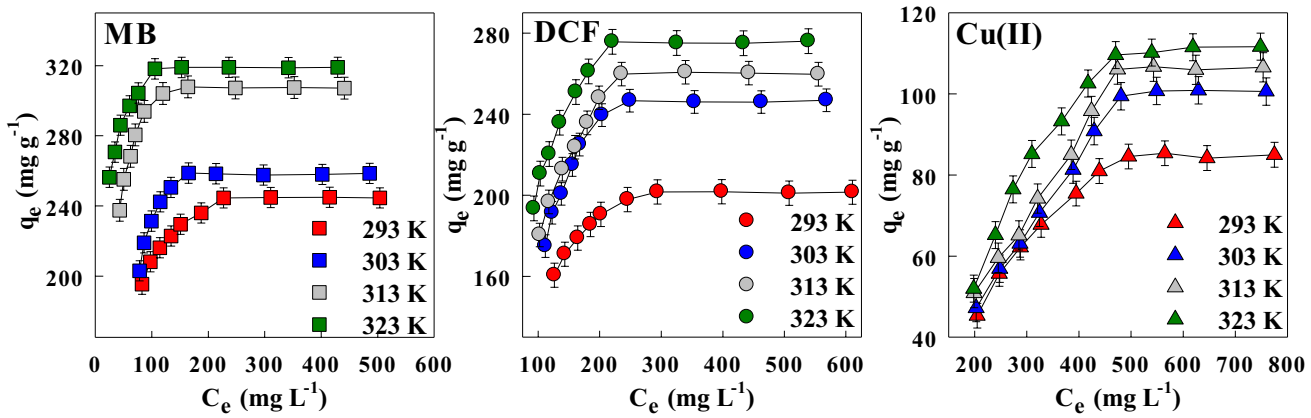

Fig. 4 Effect of temperature on the MB, DCF, and Cu(II) sorption capacity of RPAC (RPAC dosage, 50 mg; pH, 7.0 for methylene blue, 4.9 for diclofenac, and 5.0 for copper(II); interaction period, 240 min for methylene blue, 260 min for diclofenac, and 80 min for Cu(II))

Table 3 Isotherm and thermodynamic parameters of methylene blue, diclofenac, and copper(II) sorption onto RPAC

	Freundlich				Langmuir					Thermodynamics		
T	K_F	$1/n_F$	R^2	Δq(%)	q_m	K_L	R^2	R_L	Δq(%)	ΔG°	ΔH°	ΔS°
Methylene blue												
293	124.4	0.12	0.8041	6.1	256.4	0.051	0.9990	0.040	2.2	− 23.6	36.5	0.20
303	142.6	0.10	0.6256	4.9	270.3	0.069	0.9984	0.033	1.6	− 25.2		
313	181.6	0.09	0.7085	3.7	312.5	0.114	0.9994	0.020	1.1	− 27.3		
323	216.1	0.07	0.7774	3.1	322.6	0.204	0.9998	0.011	0.6	− 29.8		
Diclofenac												
293	93.3	0.13	0.7287	7.4	212.8	0.018	0.9977	0.080	2.9	− .20.9	10.3	0.11
303	82.5	0.18	0.7056	6.2	270.3	0.025	0.9942	0.076	1.8	− 22.4		
313	78.5	0.20	0.7506	4.2	285.7	0.023	0.9940	0.069	1.3	− 23.0		
323	92.6	0.19	0.7565	3.8	303.0	0.027	0.9958	0.055	0.9	− 24.1		
Copper(II)												
293	1.9	0.62	0.9080	6.9	122.0	0.002	0.9678	0.476	2.5	− 11.3	10.5	0.07
303	19.8	0.57	0.8650	4.4	185.2	0.003	0.9883	0.408	1.7	− 12.1		
313	4.2	0.47	0.8612	3.9	188.2	0.004	0.9844	0.324	1.4	− 12.5		
323	2.0	0.62	0.9079	2.6	196.1	0.005	0.9942	0.276	0.9	− 13.6		

†*T*, K; K_F, mg g^{-1} L/$mg^{-1/n}$; q_m, mg g^{-1}; K_L, L mg^{-1}; Δ*G*°, kJ mol^{-1}; Δ*H*°, kJ mol^{-1}; Δ*S*°, kJ mol^{-1} K^{-1}

The sorption isotherm parameters and R^2 were calculated from the linear plots of Langmuir (C_e/q_e vs. C_e) and Freundlich (lnq_e vs. lnC_e) (Fig. S2) drawn according to Eqs. (11) and (12) of the equilibrium data at the studied temperatures of each sorbate listed in Table 3. As can be seen from this table, the equilibrium isotherm data of the used sorbates fit the Langmuir isotherm model with higher R^2 values and lower Δ*q* (%) values than the Freundlich model. This indicates that the sorption of the sorbates used occurs as monolayer sorption on the RPAC surface that is homogeneous in sorption affinity. The Langmuir constant, K_L, of each sorbate increases with increasing temperature, indicating that the sorption affinity to the surface is greater at higher temperatures. The maximum sorption amount, q_m, determined from

Table 4 Comparison of maximum sorption capacity of methylene blue, diclofenac, and copper(II) ions of RPAC with some other biomass-based carbonaceous sorbents reported in the literature

Sorbent	Experimental conditions	q_m (mg g^{-1})	References
Methylene blue			
Tea waste, AC	25 °C, pH -	357.1	[45]
Bamboo waste, AC	40 °C, pH 4.0	1100.1	[46]
Waste palm shell, BC	–	20.0	[47]
Rice husk, BC	30 °C, pH 6.5	43.2	[48]
Rice husk, HC	30 °C, pH 6.5	11.7	[48]
Red pepper pulp,	50 °C, pH 7.0	322.6	Present study
Diclofenac			
Pinewood, BC	10 °C, pH 6.5	0.5	[49]
Pig manure, BC	10 °C, pH 6.5	12.5	[49]
Olive stone, AC	25 °C, pH 6.0	30.7	[50]
Tea waste, AC	30 °C, pH 6.5	62.5	[51]
Red pepper pulp, AC	20 °C, pH 4.9	303.0	Present study
Copper(II)			
Grape bagasse, AC	35 °C, pH 5.0	43.5	[52]
Orange waste, HC	24 °C, pH 5.0	5.8	[53]
Date seed, BC	25 °C, pH 6.0	26.7	[54]
Cow manure, BC	25 °C, pH 5.0	38.4	[55]
Grape waste	50 °C, pH 5.0	80.0	[56]
Red pepper pulp,	50 °C, pH 5.3	196.1	Present study

† *AC*, activated carbon; *BC*, biochar; *HC*, hydrochar

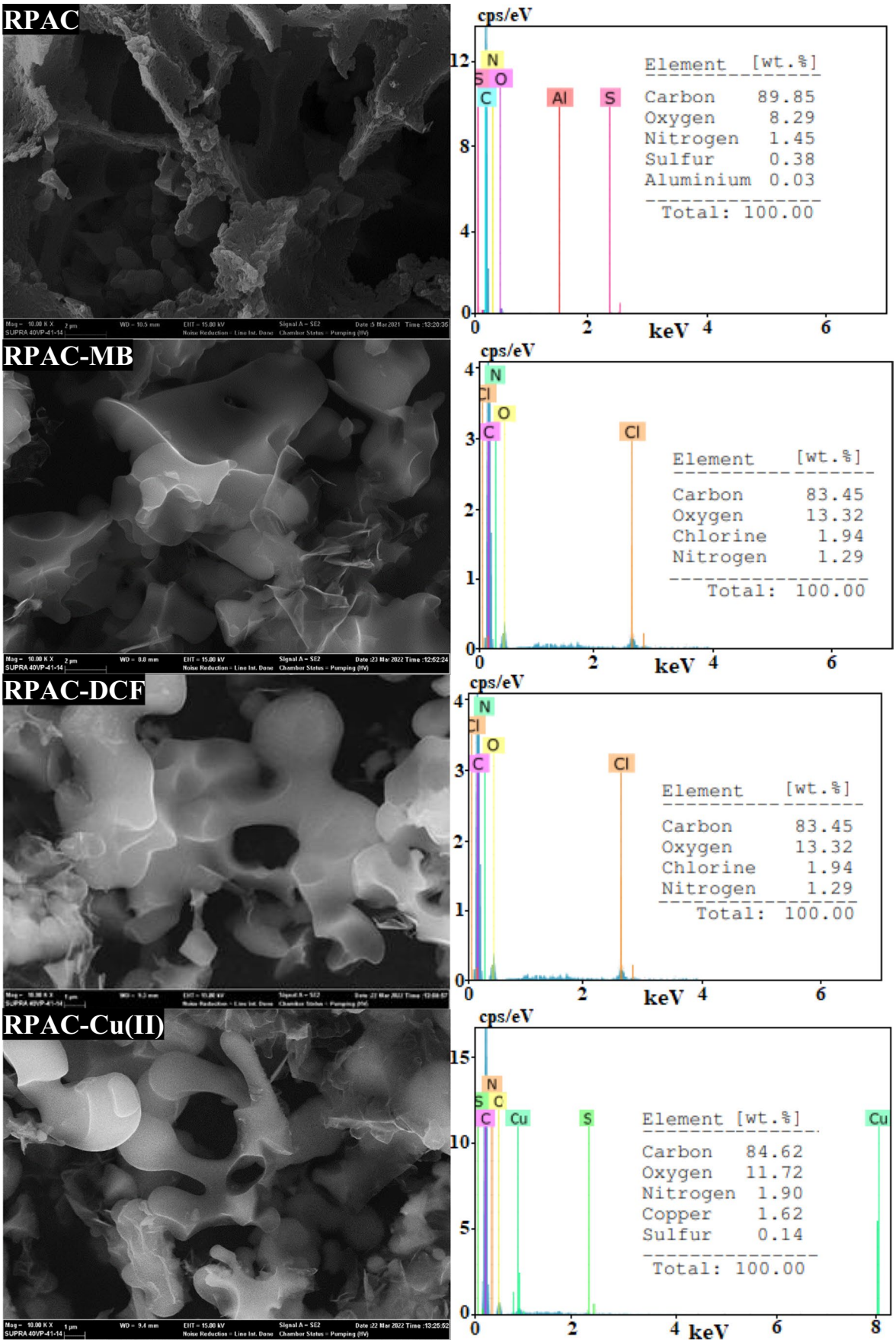
RPAC
cps/eV
Element [wt.%]
Carbon 89.85
Oxygen 8.29
Nitrogen 1.45
Sulfur 0.38
Aluminium 0.03
Total: 100.00
keV
RPAC-MB
cps/eV
Element [wt.%]
Carbon 83.45
Oxygen 13.32
Chlorine 1.94
Nitrogen 1.29
Total: 100.00
keV
RPAC-DCF
cps/eV
Element [wt.%]
Carbon 83.45
Oxygen 13.32
Chlorine 1.94
Nitrogen 1.29
Total: 100.00
keV
RPAC-Cu(II)
cps/eV
Element [wt.%]
Carbon 84.62
Oxygen 11.72
Nitrogen 1.90
Copper 1.62
Sulfur 0.14
Total: 100.00
keV

◂**Fig. 5** SEM images and EDX spectra before and after MB, DCF, and Cu(II) sorption of RPAC

the slope of the curves (Fig. S2) drawn according to the linear equation of the Langmuir model for methylene blue, diclofenac, and copper(II) was found to be 322.6, 303.0, and 196.1 mg/g at their natural pH and 50 °C, respectively. The comparison of sorption capacities used sorbates of RPAC with some other biomass-based carbonaceous sorbents reported in the literature is given in Table 4 [45–56]. From this table, it can be seen that RPAC has the capacity to sorb more methylene blue, diclofenac, and copper(II) ions than other carbon sorbents. The high sorption capacity of RPAC is due to its textural properties with a high internal surface area of 1564 $m^2\ g^{-1}$ and advanced microporous with an average diameter of 1.8 nm as seen in Table 1 as well as its surface chemical properties. The ionic sizes of methylene blue, diclofenac, and copper(II) are 0.9 nm [57], 0.81 nm [22], and 0.146 nm [55], respectively, which can easily enter its pores. Moreover, the sorption capacity of RPAC can also be explained by its surface zero charge point (pH_{PZC}) value and the surface properties at the natural pH of the used sorbates. The pH_{PZC} of the RPAC is 5.78 (Table 1). At pH < pH_{PZC}, the sorbent surface has a net positive charge, while at pH > pH_{PZC}, the surface has a net negative charge [58]. Accordingly, the surface of RPAC becomes positively charged at pH < 5.78 and negatively charged at pH > 5.78. Since the pH (7.0 for methylene blue, 4.9 for diclofenac, and 5.0 for copper(II)) studied in each sorbate sorption are larger and smaller, respectively, than the pH_{PZC} of RPAC, its surface is negatively and positively charged, respectively. The sorption of positively charged methylene blue ions and negatively charged diclofenac ions is most likely due to electrostatic attraction forces. Since the sorption of copper(II) ions is constantly repelled by the positively charged RPAC surface at the ıts natural pH, its sorption is most likely due to an ion-exchange mechanism with the protons of the protonated surface. In addition, it indicates that the R_L values (Table 3) of each sorbate at the studied temperatures are less than one, their sorption is favorable, and the fact that they are less than unity with increasing temperature increases the favorability at high temperatures. According to these values, the favorability of the sorption of the sorbates used by RPAC is methylene blue > diclofenac > copper(II), which confirms the increase in their maximum sorption capacity, q_m, in Table 3 calculated from the Langmuir equation. This fact confirms that the *1/n* values (Table 3) obtained at the investigated temperatures calculated from the Freundlich equation for all three sorbates are less than unity, confirming that their sorption is favorable.

The thermodynamic behavior of the investigated sorption systems was interpreted with thermodynamic parameters like the change in standard Gibbs free energy ($\Delta G°$, kJ mol^{-1}) mean enthalpy ($\Delta H°$, kJ mol^{-1}), and mean entropy ($\Delta S°$, kJ $mol^{-1}\ K^{-1}$). $\Delta G°$ parameters were calculated by evaluating of the Langmuir equilibrium constants, K_L derived from Langmuir linear isotherms at different temperatures in Eq. (14) [59]:

$$\Delta G^o = -RT\ln K_e^o \tag{14}$$

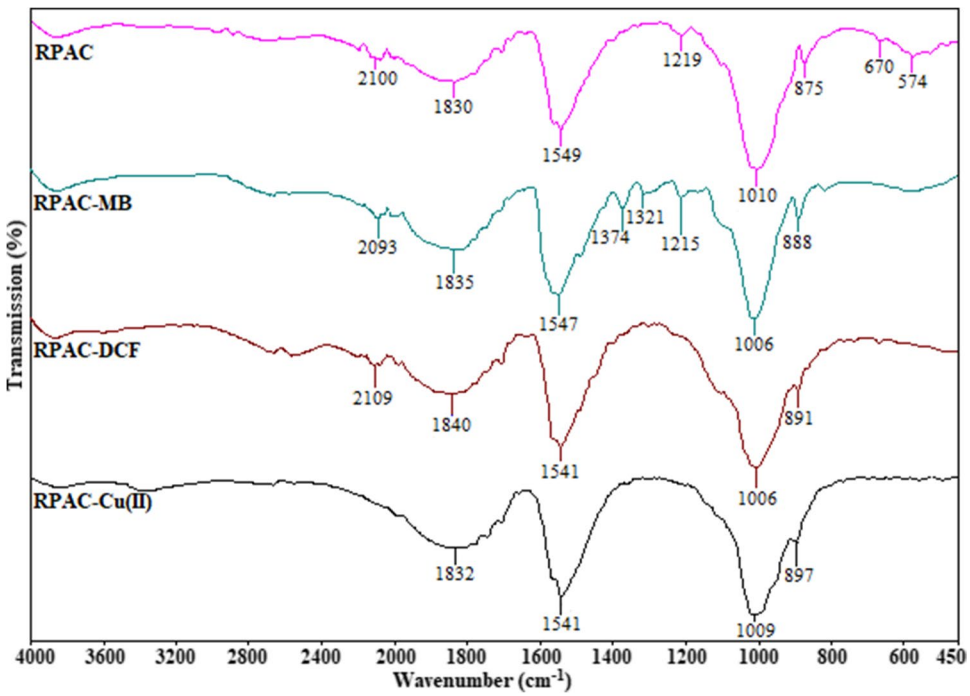

Fig. 6 FT-IR spectra of RPAC before and after MB, DCF, and Cu(II) sorption

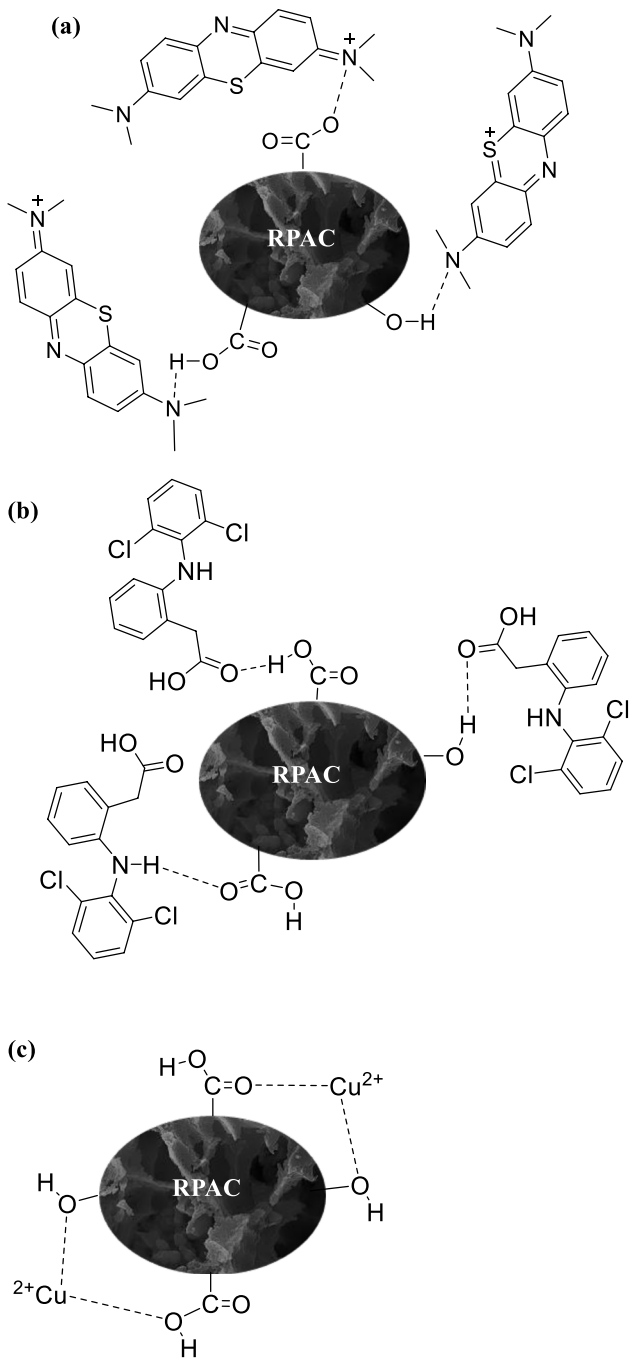

Fig. 7 Possible binding mechanism of the MB (**a**), DCF (**b**), and Cu(II) (**c**) on the RPAC

where R (8.314 J K^{-1} mol^{-1}) is the universal gas constant. T (K) is the temperature.K_2^o is the thermodynamic equilibrium constant, which was calculated from Eq. (15) [60]:

$$K_e^o = \left(1000K_L \cdot M_m\right)C^o/\gamma \tag{15}$$

where 1000 is the unit conversion factor, M_m (g mol^{-1}) is the molar mass of sorbate, $C°$ is the standard concentration of sorbate (1 mol L^{-1}), and γ is the dimensionless activity coefficient, which is about 1.0 in the case of a very diluted solution. The mean $\Delta H°$ and $\Delta S°$ values were calculated from the slope and shear values, respectively, of the graph (Fig. S3) drawn according to the van't Hoff equation given in Eq. (16):

$$\ln K_e^o = -(\Delta H^o/RT) + (\Delta S^o/R) \tag{16}$$

The $\Delta G°$ values of each sorbate at 20, 30, 40, and 50 °C were calculated as – 23.63, – 25.20, – 27.33, and – 29.77 kJ mol^{-1} for methylene blue; – 20.90, – 22.44, – 22.97, and – 24.93 kJ mol^{-1} for diclofenac; and – 11.26, – 12.08, – 12.47, and – 13.61 kJ mol^{-1} for copper(II), respectively (Table 3). The negative $\Delta G°$ values calculated for all three sorbates and the increase in their absolute values with increasing temperature indicate that their sorption is favorable and more spontaneous with increasing temperature. The mean $\Delta H°$ and $\Delta S°$ values for RPAC-methylene blue, diclofenac, and copper(II) sorption systems were calculated as 36.51, 10.31, and 10.48 kJ mol^{-1} and 0.20, 0.11, and 0.07 kJ mol^{-1} K^{-1}, respectively. The positive mean $\Delta H°$ values for the investigated sorption systems state that the processes are endothermic in nature. Furthermore, the magnitude of the $\Delta H°$ value for a sorption system gives information about whether a sorption process is physical or chemical. It is stated that the $\Delta H°$ value between 2.1 and 20.9 kJ mol^{-1} and greater for a sorption process corresponds to physical and chemical sorption, respectively [61]. This confirms that methylene blue sorption is chemical and that of diclofenac, and copper(II) ions are physical. The fact that the sorption of all three sorbates on the RPAC is an endothermic and spontaneous process as the temperature increases are also supported by the increase in q_m and K_L Langmuir isotherm parameters and the decrease in $1/n$ and R_L values (Table 3). The positive value of the mean $\Delta S°$ values indicates increased irregularity, which exhibits affinity between all three sorbates and the RPAC surface during sorption processes.

3.2 Effect of ionic strength

The effect of NaCl concentration on the sorption of methylene blue, diclofenac, and copper(II) ions by RPAC is shown in Fig. S4. The sorptions of methylene blue and diclofenac, and copper(II) increase and decrease insignificantly with increasing NaCl concentration, respectively. This is probably because the solubility of NaCl in water is higher than the sorbates used, and its affinity for the sorbent surface is less than theirs, so it does not affect their sorption.

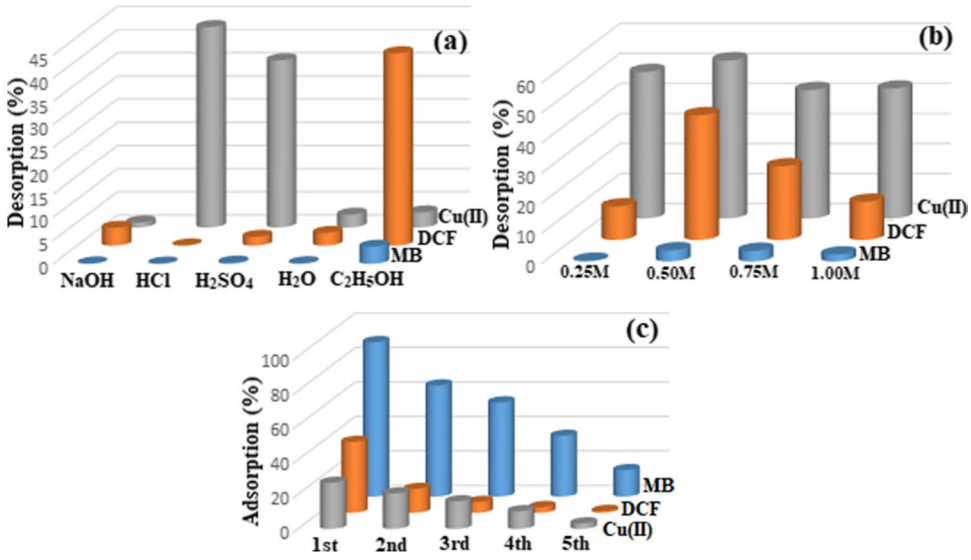

Fig. 8 Effect of different eluents on desorption efficiencies of MB, DCF, and Cu(II) (**a**); the effect of effective eluent concentrations on desorption efficiencies of MB, DCF, and Cu(II) (**b**); and regeneration cycles on MB, DCF, and Cu(II) sorption efficiencies onto RPAC (**c**)

3.3 SEM–EDX and FT-IR analysis of sorption mechanisms

Figure 5 depicts SEM images and EDX spectra of RPAC before and after sorption of each sorbate. It can be seen from SEM images that the outer surface of the RPAC, which had different sizes of voids and pores before sorption, partially filled its pores after sorption of each sorbate and also turned into light color. These may be due to the sorption of the investigated sorbates onto the RPAC surface In addition, when the EDX spectra before and after the used sorbates sorption of RPAC are examined, the presence of chlorine, which is in the structure of methylene blue and diclofenac, and copper ions indicates that the sorbates used are sorbed. Figure 6 shows the FT-IR spectra before and after the sorption of each sorbate of the RPAC. In the spectrum of RPAC, weak C≡C stretching vibration at 2100 cm^{-1}, C-H bending vibration at 1830 cm^{-1}, and C = C stretching vibration caused by aromatic ring stretching vibrations enhanced by polar functional groups at 1549 cm^{-1} observed C-O stretching due to carboxylic acid, ether, alcohol, and ester and are seen at 1219 cm^{-1}, and C–O–C asymmetric stretching vibration is seen in the structure of ether or ester at 1010 cm^{-1} [24, 62]. The peaks at 875, 670, and 574 cm^{-1} are caused by out-of-plane C-H bending vibration. There appears to be a slight shift in some spectra on diclofenac and copper(II) ion-loaded RPAC, indicating that the sorption phenomenon is physical. It is seen that both shifts and new peaks are formed in the FT-IR spectrum of methylene blue-loaded RPAC. The weak peaks at 1374 and 1321 cm^{-1} indicate the C = C stretching of the alkyl R- and C-N axial deformation of the aromatic amine, respectively [63, 64] and indicate the presence of chemically sorbed methylene blue ions. Accordingly, the binding mechanism of used sorbate ions on the RPAC could most likely be as shown in Fig. 7.

3.4 Reusability of RPAC

Figure 8a-c shows drawings of five cycle sorption–desorption processes performed with various eluents and the determined effective eluent for the reusability of RPAC relative to sorptions of the methylene blue, diclofenac, and copper(II) ions. Figure 8a shows the plots of studies on the selection of effective eluent for the desorption of used sorbates from the RPAC surface. It can be seen from this figure that the effective eluent for the desorption of methylene blue, diclofenac, and copper(II) ions is C_2H_5OH and HCl, respectively. Figure 8b depicts plots for determining the effective concentrations of the active eluents identified in Fig. 8a, which show 0.50 M C_2H_5OH, C_2H_5OH, and HCl for used sorbates, respectively. Figure 8c demonstrates plots of five cyclic reusability studies at the active eluent and their effective concentrations determined in Fig. 8a and b for each sorbate. It can be seen from this figure that the sorption effectiveness of RPAC for all three sorbates decreased after three cycles. This decrease is probably due to the fact that active sorption sites on the RPAC surface gradually lose their activity with increasing cycle numbers.

4 Conclusion

In this study, the performance of industrially processed red pepper pulp-based activated carbon to remove methylene blue, diclofenac, and copper(II) ions selected as sorbate

from aqueous solutions was investigated physicochemically. The sorption of examined sorbates increased with the rise of interaction period, initial sorbate concentration, and solution temperature while decreasing with the increase in RPAC dosage. Moreover, the sorption of methylene blue, diclofenac, and copper(II) ions increased and decreased insignificantly with increasing NaCl concentration, respectively. The kinetic data obtained at the initial concentrations at diverse time intervals for each sorbate are well defined by the PSO model which is supported by the fact that the experimental sorbed amounts are consistent with the calculated ones, with high R^2 and low $\Delta q\%$ values. The rate-controlling in the sorption mechanism of each sorbate is not only the IPD stage but the others also affected. The equilibrium data at the temperatures studied for each sorbate best fit the Langmuir isotherm model, with higher R^2 and low $\Delta q\%$ values than the Freundlich model. The maximum sorption amounts for methylene blue, diclofenac, and copper(II) ions by RPAC were 322.6, 303.0, and 196.1 mg g^{-1} at their natural pH and 50 °C, respectively. The Langmuir R_L separation factors and Freundlich $1/n$ constants calculated for each sorption system were found to be in the range of 0.0–1.0 and less than 1.0, respectively, indicating that the sorption processes are positive. The thermodynamic parameters computed for each sorption system specified that the sorption processes were endothermic and spontaneous in nature. Reusability studies demonstrated that RPAC can be used for up to three cycles for each sorbate with high sorption efficiency.

In conclusion, current research results show that RPAC can be used as an effective sorbent as an alternative to commercial sorbents to reduce pollutants from water.

Supplementary information The online version contains supplementary material available at https://doi.org/10.1007/s13399-022-03677-6.

Author contribution Filiz Koyuncu, data curation, methodology, visualization, investigation, formal analysis, and writing, original draft preparation. Fuat Güzel, conceptualization; methodology; writing, review and editing; software; writing, original draft preparation; supervision; software; validation; and project administration. Yekbun Avşar Teymur, data curation; methodology; writing, review and editing; visualization; and investigation.

Funding This study was supported by the Scientific Research Projects Coordinator of Dicle University (Grant No.: ZGEF.19.006).

Data availability Not applicable.

Code availability Not applicable.

Declarations

Ethical approval Not applicable. This article does not contain any studies with human participants or animals performed by any of the authors.

Consent to participate Not applicable.

Consent for publication The authors confirm that the final version of the manuscript has been reviewed, approved, and consented for publication by all authors.

Competing interests The authors declare no competing interests.

References

1. Chieng HI, Lim LB, Priyantha N (2015) Enhancing adsorption capacity of toxic malachite green dye through chemically modified breadnut peel: equilibrium, thermodynamics, kinetics and regeneration studies. Environ Technol 36:86–97. https://doi.org/10.1080/09593330.2014.938124
2. Chen WH, Hoang AT, Nižetić S, Pandey A, Cheng CK, Luque R, Ongm HC, Thomas S, Nguyen XP (2022) Biomass-derived biochar: from production to application in removing heavy metal-contaminated water. Process Saf Environ Prot 160:704–733. https://doi.org/10.1016/j.psep.2022.02.061
3. Mokhtari P, Ghaedi M, Dashtian K, Rahimi MR, Purkait MK (2016) Removal of methyl orange by copper sulfide nanoparticles loaded activated carbon: kinetic and isotherm investigation. J Mol Liq 219:299–305. https://doi.org/10.1016/j.molliq.2016.03.022
4. Amusat SO, Kebede TG, Dube S, Nindi MM (2021) Ball-milling synthesis of biochar and biochar–based nanocomposites and prospects for removal of emerging contaminants: a review. J Water Process Eng 41:101993. https://doi.org/10.1016/j.jwpe.2021.101993
5. Barquilha CE, Braga MC (2021) Adsorption of organic and inorganic pollutants onto biochars: challenges, operating conditions, and mechanisms. Bioresour Technol Rep 15:100728. https://doi.org/10.1016/j.biteb.2021.100728
6. Zhang L, Li W, Cao H, Hu D, Chen X, Guan Y, Tang J, Gao H (2019) Ultra-efficient sorption of Cu2+ and Pb2+ ions by light biochar derived from *Medulla tetrapanacis*. Bioresour Technol 291:121818. https://doi.org/10.1016/j.biortech.2019.121818
7. Katiyar R, Patel AK, Nguyen TB, Singhania RR, Chen CW, Dong CD (2021) Adsorption of copper (II) in aqueous solution using biochars derived from *Ascophyllum nodosum* seaweed. Bioresour Technol 328:124829. https://doi.org/10.1016/j.biortech.2021.124829
8. Ali J, Bakhsh EM, Hussain N, Bilal M, Akhtar K, Fagieh TM, Danish EY, Asiri AM, Su X, Khan SB (2022) A new biosource for synthesis of activated carbon and its potential use for removal of methylene blue and eriochrome black T from aqueous solutions. Ind Crops Prod 179:114676. https://doi.org/10.1016/j.indcrop.2022.114676
9. Lima DR, Hosseini-Bandegharaei A, Thue PS, Lima EC, de Albuquerque YR, dos Reis GS, Umpierres CS, Dias SLP, Tran HN (2019) Efficient acetaminophen removal from water and hospital effluents treatment by activated carbons derived from Brazil nutshells. Colloids Surf A: Physicochem Eng Asp 583:123966. https://doi.org/10.1016/j.colsurfa.2019.123966
10. González-García P (2018) Activated carbon from lignocellulosic precursors: a review of the synthesis methods, characterization techniques and applications. Renew Sust Energ Rev 82:1393–1414. https://doi.org/10.1016/j.rser.2017.04.117
11. Prakash MO, Raghavendra G, Ojha S, Panchal M (2021) Characterization of porous activated carbon prepared from arhar stalks by single step chemical activation method. Mater Today Proc 39:1476–1481. https://doi.org/10.1016/j.matpr.2020.05.370
12. Zhang J, Zhang W, Zhang H, Pang J, Cao G, Han M, Yang Y (2017) Facile preparation of water soluble phenol formaldehyde resin-derived activated carbon by Na_2CO_3 activation for high performance supercapacitors. Mater Lett 206:67–70. https://doi.org/10.1016/j.matlet.2017.06.091

13. Shen Y, Fu Y (2018) KOH-activated rice husk char via CO_2 pyrolysis for phenol adsorption. Mater Today Energy 9:397–405. https://doi.org/10.1016/j.mtener.2018.07.005
14. Canales-Flores RA, Prieto-García F (2020) Taguchi optimization for production of activated carbon from phosphoric acid impregnated agricultural waste by microwave heating for the removal of methylene blue. Diam Relat Mater 109:108027. https://doi.org/10.1016/j.diamond.2020.108027
15. Okolie JA, Nanda S, Dalai AK, Kozinski JA (2021) Chemistry and specialty industrial applications of lignocellulosic biomass. Waste Biomass Valor 12:2145–2169. https://doi.org/10.1007/s12649-020-01123-0
16. Abdulhameed AS, Hum NNMF, Rangabhashiyam S, Jawad AH, Wilson LD, Yaseen ZM, Al-Kahtani AA, Alothman ZA (2021) Statistical modeling and mechanistic pathway for methylene blue dye removal by high surface area and mesoporous grass-based activated carbon using K_2CO_3 activator. J Environ Chem Eng 9:105530. https://doi.org/10.1016/j.jece.2021.105530
17. Lazarotto JS, da Boit MK, Georgin J, Franco DS, Netto MS, Piccilli DG, Silva LFO, Lima ED, Dotto GL (2021) Preparation of activated carbon from the residues of the mushroom (*Agaricus bisporus*) production chain for the adsorption of the 2, 4-dichlorophenoxyacetic herbicide. J Environ Chem Eng 9:106843. https://doi.org/10.1016/j.jece.2021.106843
18. Siraorarnroj S, Kaewtrakulchai N, Fuji M, Eiad-ua A (2022) High performance nanoporous carbon from mulberry leaves (Morus alba L) residues via microwave treatment assisted hydrothermal-carbonization for methyl orange adsorption: kinetic, equilibrium and thermodynamic studies. Materialia 21:101288. https://doi.org/10.1016/j.mtla.2021.101288
19. Zhou C, Wang Y (2020) Recent progress in the conversion of biomass wastes into functional materials for value-added applications. Sci Technol Adv Mater 21:787–804. https://doi.org/10.1080/14686996.2020.1848213
20. Saadi W, Rodríguez-Sánchez S, Ruiz B, Najar-Souissi S, Ouederni A, Fuente E (2022) From pomegranate peels waste to one-step alkaline carbonate activated carbons Prospect as sustainable adsorbent for the renewable energy production. J Environ Chem Eng 10:107010. https://doi.org/10.1016/j.jece.2021.107010
21. Uddin MT, Islam MA, Mahmud S, Rukanuzzaman M (2009) Adsorptive removal of methylene blue by tea waste. J Hazard Mater 164:53–60. https://doi.org/10.1016/j.jhazmat.2008.07.131
22. Li Y, Taggart MA, McKenzie C, Zhang Z, Lu Y, Pap S, Gibb S (2019) Utilizing low-cost natural waste for the removal of pharmaceuticals from water: Mechanisms, isotherms and kinetics at low concentrations. J Clean Prod 227:88–97. https://doi.org/10.1016/j.jclepro.2019.04.081
23. Hiew BYZ, Lee LY, Lee XJ, Gan S, Thangalazhy-Gopakumar S, Lim SS, Pan GT, Yang TCK (2019) Adsorptive removal of diclofenac by graphene oxide: optimization, equilibrium, kinetic and thermodynamic studies. J Taiwan Inst Chem Eng 98:150–162. https://doi.org/10.1016/j.jtice.2018.07.034
24. Koyuncu F, Güzel F, İnal İIG (2022) High surface area and supermicroporous activated carbon from capsicum (Capsicum annuum L.) industrial processing pulp via single-step KOH-catalyzed pyrolysis: production optimization, characterization and its some water pollutants removal and supercapacitor performance. Diam Relat Mater 124:108920. https://doi.org/10.1016/j.diamond.2022.108920
25. Ahmed MJ, Islam MA, Asif M, Hameed BH (2017) Human hair-derived high surface area porous carbon material for the adsorption isotherm and kinetics of tetracycline antibiotics. Bioresour Technol 243:778–784. https://doi.org/10.1016/j.cej.2016.10.065
26. Lu Z, Zhang H, Shahab A, Zhang K, Zeng H, Nabi I, Ullah H (2021) Comparative study on characterization and adsorption properties of phosphoric acid activated biochar and nitrogen-containing modified biochar employing Eucalyptus as a precursor. J Clean Prod 303:127046. https://doi.org/10.1016/j.jclepro.2021.127046
27. Shen Z, Jin F, Wang F, McMillan O, Al-Tabbaa A (2015) Sorption of lead by Salisbury biochar produced from British broadleaf hardwood. Bioresour Technol 193:553–556. https://doi.org/10.1016/j.biortech.2015.06.111
28. Sun T, Xu Y, Sun Y, Wang L, Liang X, Jia H (2021) Crayfish shell biochar for the mitigation of Pb contaminated water and soil: characteristics, mechanisms, and applications. Environ Pollut 271:116308. https://doi.org/10.1016/j.envpol.2020.116308
29. Gohr MS, Abd-Elhamid AI, El-Shanshory AA, Soliman HM (2022) Adsorption of cationic dyes onto chemically modified activated carbon: Kinetics and thermodynamic study. J Mol Liq 346:118227. https://doi.org/10.1016/j.molliq.2021.118227
30. Chen S, Zhang J, Zhang C, Yue Q, Li Y, Li C (2010) Equilibrium and kinetic studies of methyl orange and methyl violet adsorption on activated carbon derived from *Phragmites australis*. Desalination 252:149–156. https://doi.org/10.1016/j.desal.2009.10.010
31. Wang L (2012) Application of activated carbon derived from 'waste' bamboo culms for the adsorption of azo disperse dye: kinetic, equilibrium and thermodynamic studies. J Environ Manage 102:79–87. https://doi.org/10.1016/j.jenvman.2012.02.019
32. Saremi F, Miroliaei MR, Nejad MS, Sheibani H (2020) Adsorption of tetracycline antibiotic from aqueous solutions onto vitamin B6-upgraded biochar derived from date palm leaves. J Mol Liq 318:114126. https://doi.org/10.1016/j.molliq.2020.114126
33. Lagergren S (1898) About the theory of so-called adsorption of soluble substance. Kungliga Sven VetenskapsakademiensHandl 24:1–39
34. Ho YS, McKay G (1998) Kinetic models for the sorption of dye from aqueous solution by wood. Process Saf Environ Prot 76:183–191. https://doi.org/10.1205/095758298529326
35. Cheira MF, Kouraim MN, Zidan IH, Mohamed WS, Hassanein TF (2020) Adsorption of U(VI) from sulfate solution using montmorillonite/polyamide and nano-titanium oxide/polyamide nanocomposites. J Environ Chem Eng 8:104427. https://doi.org/10.1016/j.jece.2020.104427
36. Weber WJ, Morris JC (1963) Kinetics of adsorption on carbon from solution. J Saint Eng Div Am Soc Civil Eng 89:31–60. https://doi.org/10.1061/JSEDAI.0000430
37. Ahmed MJ, Theydan SK (2012) Adsorption of cephalexin onto activated carbons from *Albizia lebbeck* seed pods by microwave-induced KOH and K_2CO_3 activations. Chem Eng J 211:200–207. https://doi.org/10.1016/j.cej.2012.09.089
38. Sekulic MT, Boskovic N, Slavkovic A, Garunovic J, Kolakovic S, Pap S (2019) Surface functionalised adsorbent for emerging pharmaceutical removal: adsorption performance and mechanisms. Process Saf Environ 125:50–63. https://doi.org/10.1016/j.psep.2019.03.007
39. Gao Y, Yue Q, Gao B, Sun Y, Wang W, Li Q, Wang Y (2013) Comparisons of porous, surface chemistry and adsorption properties of carbon derived from *Enteromorpha prolifera* activated by $H_4P_2O_7$ and KOH. Chem Eng J 232:582–590. https://doi.org/10.1016/j.cej.2013.08.011
40. Chen Y, Zhai SR, Liu N, Song Y, An QD, Song XW (2013) Dye removal of activated carbons prepared from NaOH-pretreated rice husks by low-temperature solution-processed carbonization and H_3PO_4 activation. Bioresour Technol 144:401–409. https://doi.org/10.1016/j.biortech.2013.07.002
41 Langmuir I (1989) The adsorption of gases on plane surfaces of glass, mica and platinum. J Am Chem Soc 40:1361–1403. https://doi.org/10.1021/ja02242a004
42. Freundlich H (1906) Over the adsorption in solutions. Z Phys Chem 57:385–470. https://doi.org/10.1515/zpch-1907-5723
43. Isa MH, Lang LS, Asaari FA, Aziz HA, Ramli NA, Dhas JPA (2007) Low cost removal of disperse dyes from aqueous

solution using palm ash. Dyes Pigments 74:446–453. https://doi.org/10.1016/j.dyepig.2006.02.025
44. Ji B, Wang J, Song H, Chen W (2019) Removal of methylene blue from aqueous solutions using biochar derived from a fallen leaf by slow pyrolysis: behavior and mechanism. J Environ Chem Eng 7:103036. https://doi.org/10.1016/j.jece.2019.103036
45. Tuli FJ, Hossain A, Kibria AF, Tareq ARM, Mamun SM, Ullah A (2020) Removal of methylene blue from water by low-cost activated carbon prepared from tea waste: a study of adsorption isotherm and kinetics. Environ Nanotechnol Monit Manag 14:100354. https://doi.org/10.1016/j.enmm.2020.100354
46. Wang Y, Srinivasakannan C, Wang H, Xue G, Wang L, Wang X, Duan X (2022) Preparation of novel biochar containing graphene from waste bamboo with high methylene blue adsorption capacity. Diam Relat Mater 125:109034. https://doi.org/10.1016/j.diamond.2022.109034
47. Kong SH, Lam SS, Yek PNY, Liew RK, Ma NL, Osman MS, Wong CC (2019) Self-purging microwave pyrolysis: an innovative approach to convert oil palm shell into carbon-rich biochar for methylene blue adsorption. J Chem Technol Biotechnol 94:1397–1405. https://doi.org/10.1002/jctb.5884
48. Lang J, Matějová L, Cuentas-Gallegos AK, Lobato-Peralta DR, Ainassaari K, Gómez MM, Solís JL, Mondal D, Keiski RL, Cruz GJ (2021) Evaluation and selection of biochars and hydrochars derived from agricultural wastes for the use as adsorbent and energy storage materials. J Environ Chem Eng 9:105979. https://doi.org/10.1016/j.jece.2021.105979
49. Lonappan L, Rouissi T, Brar SK, Verma M, Surampalli RY (2018) An insight into the adsorption of diclofenac on different biochars: mechanisms, surface chemistry, and thermodynamics. Bioresour Technol 249:386–394. https://doi.org/10.1016/j.biortech.2017.10.039
50. Cherik D, Louhab K (2018) A kinetics, isotherms, and thermodynamic study of diclofenac adsorption using activated carbon prepared from olive stones. J Disper Sci Technol 39:814–825. https://doi.org/10.1080/01932691.2017.1395346
51. Malhotra M, Sures S, Garg A (2018) Tea waste derived activated carbon for the adsorption of sodium diclofenac from wastewater: adsorbent characteristics, adsorption isotherms, kinetics, and thermodynamics. Environ Sci Pollut Res 25:32210–32220. https://doi.org/10.1007/s11356-018-3148-y
52. Demiral H, Güngör C (2016) Adsorption of copper (II) from aqueous solutions on activated carbon prepared from grape bagasse. J Clean Prod 124:103–113. https://doi.org/10.1016/j.jclepro.2016.02.084
53. Pellera FM, Giannis A, Kalderis D, Anastasiadou K, Stegmann R, Wang JY, Gidarakos E (2012) Adsorption of Cu (II) ions from aqueous solutions on biochars prepared from agricultural by-products. J Environ Manage 96:35–42. https://doi.org/10.1016/j.jenvman.2011.10.010
54. Mahdi Z, Yu QJ, El Hanandeh A (2018) Investigation of the kinetics and mechanisms of nickel and copper ions adsorption from aqueous solutions by date seed derived biochar. J Environ Chem Eng 6:1171–1181. https://doi.org/10.1016/j.jece.2018.01.021
55. Zhang P, Zhang X, Yuan X, Xie R, Han L (2021) Characteristics, adsorption behaviors, Cu (II) adsorption mechanisms by cow manure biochar derived at various pyrolysis temperatures. Bioresour Technol 331:125013. https://doi.org/10.1016/j.biortech.2021.125013
56. Güzel F, Sayğılı GA, Sayğılı H, Koyuncu F, Kaya N, Güzel S (2021) Performance of grape (*Vitis vinifera* L.) industrial processing solid waste–derived nanoporous carbon in copper (II) removal. Biomass Convers Biorefining 11:1363–1373. https://doi.org/10.1007/s13399-020-00787-x
57. Güzel F (1996) The effect of surface acidity upon the adsorption capacities of activated carbons. Separ Sci Technol 31:283–290. https://doi.org/10.1080/01496399608000696
58. Al-Degs Y, Khraisheh MAM, Allen SJ, Ahmad MN (2000) Effect of carbon surface chemistry on the removal of reactive dyes from textile effluent. Water Res 34:927–935. https://doi.org/10.1016/S0043-1354(99)00200-6
59. Bachmann SAL, Calvete T, Féris LA (2021) Caffeine removal from aqueous media by adsorption: an overview of adsorbents evolution and the kinetic, equilibrium and thermodynamic studies. Sci Total Environ 767:144229. https://doi.org/10.1016/j.scitotenv.2020.144229
60. Lima EC, Hosseini-Bandegharaei A, Moreno-Piraján JC, Anastopoulos I (2019) A critical review of the estimation of the thermodynamic parameters on adsorption equilibria. Wrong use of equilibrium constant in the Van't Hoof equation for calculation of thermodynamic parameters of adsorption. J Mol Liq 273:425–434. https://doi.org/10.1016/j.molliq.2018.10.048
61. Anayurt RA, Sari A, Tuzen M (2009) Equilibrium, thermodynamic and kinetic studies on biosorption of Pb (II) and Cd (II) from aqueous solution by macrofungus (*Lactarius scrobiculatus*) biomass. Chem Eng J 151:255–261. https://doi.org/10.1016/j.cej.2009.03.002
62. Puziy AM, Poddubnaya OI, Martınez-Alonso A, Suárez-Garcıa F, Tascón JMD (2002) Synthetic carbons activated with phosphoric acid: I. Surface chemistry and ion binding properties. Carbon 40:1493–1505. https://doi.org/10.1016/S0008-6223(01)00317-7
63. Auta M, Hameed BH (2014) Chitosan–clay composite as highly effective and low-cost adsorbent for batch and fixed-bed adsorption of methylene blue. Chem Eng J 237:352–361. https://doi.org/10.1016/j.cej.2013.09.066
64. Chen C, Fu Q, Chen X, He G, Ye J, Zhou C, Hu K, Cheng L, Zhao M (2022) An effective pre-burning treatment boosting adsorption capacity of sorghum distillers' grain derived porous carbon. Diam Relat Mater 124:108914. https://doi.org/10.1016/j.diamond.2022.108914